Journal of Applied Electrochemistry **29**: 463–471, 1999.

Electrochemical impedance studies of a decade-aged magnesium/manganese dioxide primary cell

N. MUNICHANDRAIAH
Department of Inorganic and Physical Chemistry, Indian Institute of Science, Bangalore 560 012, India (e-mail: muni@ipc.iisc.ernet.in; fax: +91 80 3341683)

Received 25 June 1998; accepted in revised form 13 October 1998

Key words: a.c. impedance, discharge delay-time, Mg/MnO_2 primary cell, state-of-charge, surface passive film on Mg

Abstract

A Mg/MnO_2 primary cell yields specific energy higher than a conventional Zn/MnO_2 cell. Additionally, the shelf life of the Mg/MnO_2 cell is extremely high. These cells, which were more than a decade old, were investigated for their discharge capacity, delay-time behaviour and impedance characteristics. The values of discharge capacity and the delay-time of an aged Mg/MnO_2 cell were comparable to those of a fresh cell. The voltage dip on initiation of a galvanostatic current, however, was rather large. This was attributed to the presence of a thick, and highly resistive, surface passive film on the Mg anode. The complex plane electrochemical impedance spectrum of a partially discharged cell consisted of two semicircles whose sizes decreased with decrease of state-of-charge of the cell. The a.c. frequency corresponding to the maximum value of the imaginary part of the high frequency semicircle was shown to be a useful parameter for estimation of the state-of-charge of the cell. The resistance parameters of a partially discharged Mg/MnO_2 cell increased linearly with open circuit ageing time. This feature was attributed to growth of a passive surface layer on the Mg anode.

1. Introduction

The magnesium/manganese dioxide primary cell possesses superior performance characteristics in comparison with the conventional zinc/manganese dioxide primary cell [1]. The basic difference between these two cell systems lies in the electrochemistry of the anode material, while the electrochemistry of the cathode material, that is, manganese dioxide remains the same. By virtue of high standard electrode potential (−2.37 V), low density (7.44 g cm^{-3}) and high electrochemical specific capacity (2.2 Ah g^{-1}) of the magnesium anode, the energy output per unit weight or unit volume of a Mg/MnO_2 cell is much higher than that of a Zn/MnO_2 cell. Furthermore, the shelf life of the Mg/MnO_2 cell is also higher by several times than that of the Zn/MnO_2 cell. The high shelf life is attributed to the presence of passive oxide film on the Mg anode. The passive film prevents corrosion of the Mg metal by the cell electrolyte, thus protecting the cell from pore formation due to localized corrosion and leaking of the electrolyte. It also behaves as a barrier between the anode and the cathode, and prevents any possible self-discharge. As a result, the Mg/MnO_2 cell can be stored over several years without loss of capacity.

In the present investigations Mg/MnO_2 cells, which were more than a decade old and had been stored in an ambient laboratory environment, were investigated for their electrochemical characteristics.

2. Experimental details

The Mg/MnO_2 cells of CD-size were manufactured by Bharat Electronics, India. Mg–AZ21 alloy, in the form of a can, served both as the anode material and the cell container. The cathode material consisted of a blend of MnO_2 and acetylene black in an aqueous electrolyte of magnesium perchlorate. The anode and the cathode were separated by kraft paper. These cells were manufactured around 1985 and some of them were used for studies previously reported from this laboratory [2–4].

Several of these cells were stored since then in sealed polythene bags in the laboratory environment at ambient temperature.

The cells were characterized using an electrochemical impedance analyser (EG&G Parc model 6310) for impedance studies, and a galvanostat/potentiostat (EG&G Parc model Versastat) for delay-time and cell discharge studies. These instruments were driven by an IBM compatible computer. A galvanostatic circuit consisting of a regulated d.c. power source in series with a high resistance and an ammeter, was also employed for some cell discharge studies. Some commercial D-size Zn/MnO_2 cells were also discharged for comparison. Electrochemical impedance spectra of the cells were recorded at several states-of-charge by an excitation signal of 5 mV in the a.c. frequency range of 100 kHz–100 mHz. Time variation of the impedance data was recorded for partially discharged cells. Experiments were carried out at 20 ± 1 °C, and with several cells to ensure reproducibility.

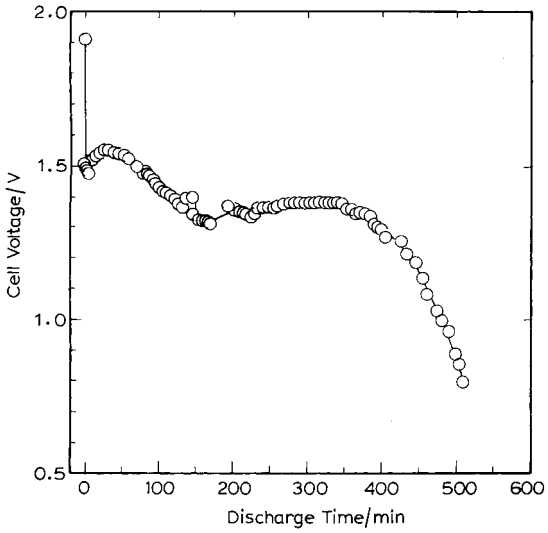

Fig. 1. Variation of voltage of a decade-aged Mg/MnO_2 cell during galvanostatic discharge at a current of 0.3 A.

3. Results and discussion

Although the Mg/MnO_2 cells were manufactured more than a decade ago, they were found to have good physical appearance. The cells were partially covered with a thin and transparent polymer film since the time they were assembled. The outer surface of the Mg remained clean without any perforations or electrolyte leakage. This is attributable to the uniform and coherent passive film present on the Mg surface, which resists localized pitting corrosion of Mg metal by the cell electrolyte, as well as by the external environment.

3.1. *Cell discharge*

During discharge of a Mg/MnO_2 cell, the following reactions take place: at the anode

$$Mg \rightarrow Mg^{2+} + 2e^- \quad (1)$$

at the cathode

$$MnO_2 + H_2O + e^- \rightarrow MnOOH + OH^- \quad (2)$$

$$MnOOH + H_2O + e^- \rightarrow Mn(OH)_2 + OH^- \quad (3)$$

Reaction 1 is irreversible and Mg^{2+} ions produced may be converted into $Mg(OH)_2$ by combination with OH^- ions produced at the cathode in Reactions 2 and 3.

A typical galvanostatic discharge curve of a Mg/MnO_2 cell is shown in Figure 1. A discharge capacity of 2.5 Ah was obtained at a discharge current of 0.3 A and a cut off voltage of 0.8 V. This capacity value is nearly the same as that for a fresh cell [2]. These results suggest that there is no appreciable loss of capacity during long storage of the cell. Figure 2 shows the energy density as a function of the power density. Data for commercial D-size Zn/MnO_2 cells are also presented in Figure 2 for the purpose of comparison. It is interesting to note that the performance of the aged Mg/MnO_2 cells is far superior.

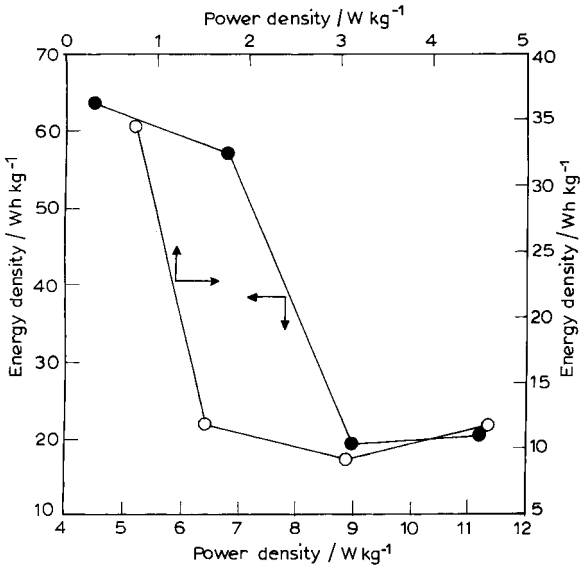

Fig. 2. Energy density of an aged Mg/MnO_2 cell (●) and a commercial Zn/MnO_2 cell (○) as a function of the power density.

3.2. *Delay-time of Mg/MnO_2 cell*

When a Mg/MnO_2 cell is subjected to galvanostatic discharge, the cell voltage initially dips to a low value before reaching the normal closed circuit voltage. The time lag, known as the delay-time, is a unique feature of Mg-based primary cells. A voltage transient recorded at the beginning of cell discharge by a 0.2 A discharge current is shown in Figure 3. The cell voltage prior to discharge was 1.91 V, and decreased to −2.05 V instantaneously (0.06 s). Following this, the cell voltage increased and reached 1.56 V in 2.42 s; 1.62 V in 5 s and a maximum of 1.66 V in 30 s. The delay-time of 2.42 s was marginally greater than the 1.5 s reported for a fresh cell [5]. However, a pronounced effect of storing the cells over several years was reflected in the large voltage fall. There was a fall of 3.96 V from 1.91 to −2.05 V in the present experiments, whereas about 0.45 V was reported for a fresh cell [5].

The presence of a passive film on the Mg anode surface is responsible for the delay-time of the Mg/MnO_2 cell [5]. It is believed that the passive film does not readily allow the current to flow through the cell instantaneously on closing the discharge circuit. The breakdown of the passive film is an essential prerequisite for a continuous flow of current through the cell. The large voltage drop (Figure 3) is due to a thick and resistive passive film grown on the Mg anode during several years of storage.

3.3. *Electrochemical impedance spectroscopy at different states-of-charge*

The cathode of Mg/MnO_2 cell, consisting of MnO_2 particles mixed with acetylene black is porous and has a specific surface area several times greater than that of the Mg anode. It has been reported that the impedance of high surface area MnO_2 cathode of a Leclanche cell is negligibly smaller than that of the anode and the cell impedance is, therefore, attributable to the impedance of the anode itself [6]. The equivalent circuit of the Mg anode is shown in Figure 4(a). The ohmic resistance of the cell is shown as R_Ω. Since the Mg anode is covered with a surface film, the film resistance (R_f) and its capacitance (C_f) are considered in a parallel combination. The charge-transfer resistance (R_{ct}), the diffusion-limited Warburg impedance (W), and the double-layer capacitance (C_{dl}) are included according to the Randles equivalent circuit model [7]. As the a.c. impedance experiments were performed with an excitation signal of 5 mV at open circuit conditions, equilibrium conditions of the cell are considered. Since the Mg metal is not reversible with respect to Mg^{2+} ions, it is considered to be under corrosion by the following reactions:

$$Mg \rightarrow Mg^{2+} + 2e^- \quad (1)$$

$$2H^+ + 2e^- \rightarrow H_2 \quad (4)$$

resulting in an overall reaction:

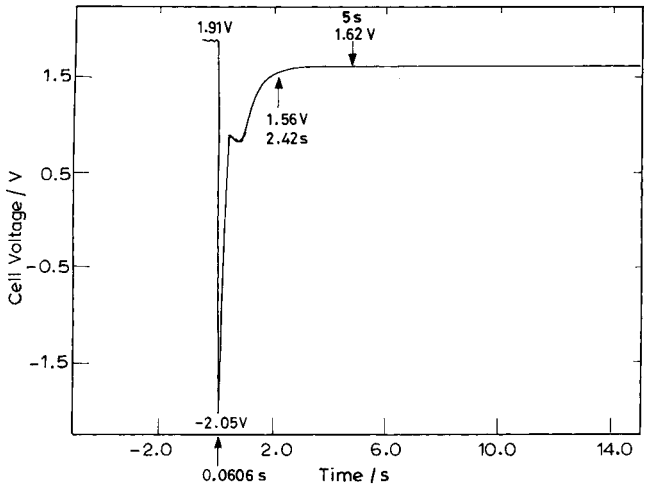

Fig 3. Voltage transient of a Mg/MnO_2 cell recorded on initiation of 0.2 A discharge current.

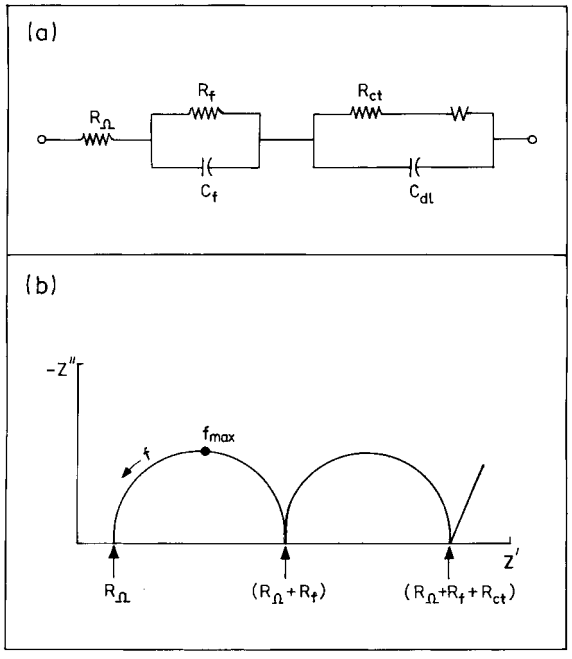

Fig. 4. The equivalent circuit of Mg anode in Mg/MnO_2 cell (a), and corresponding complex plane diagram of a.c. impedance (b). R_Ω is ohmic resistance of the cell, R_f and C_f are resistance and capacitance of surface passive film on Mg anode, R_{ct} is charge-transfer resistance of Mg corrosion process, C_{dl} is double-layer capacitance and W is Warburg impedance.

$$Mg + 2\,H^+ \rightleftharpoons Mg^{2+} + H_2 \quad (5)$$

Thus, R_{ct} shown in Figure 4 corresponds to Reaction 5.

A schematic Nyquist plot, which is expected for the equivalent circuit, is shown in Figure 4(b). The high frequency intercept of the impedance plot provides the value of ohmic resistance (R_Ω) of the cell. The value of R_f can be evaluated from the diameter of the high frequency semi circle, and film capacitance C_f from the following relationship:

$$C_f = 1/(2\pi f_{max} R_f) \quad (6)$$

where f_{max} is the a.c. frequency corresponding to the maximum in the imaginary component (Z'') on the semi circle. In a similar way, the charge-transfer resistance (R_{ct}) and the double-layer capacitance (C_{dl}) of the Mg electrode can be obtained from the low frequency semicircle.

Before being subjected to discharge, Mg/MnO_2 cells were found to have extremely high resistance by a.c. impedance measurements. The impedance spectrum in Nyquist and Bode forms is shown in Figure 5. The frequency dispersion of the spectrum (Figure 5(a)) did not appear as a semicircle, or a pair of semicircles, as discussed earlier. The modulus of impedance ($|Z|$) at low frequency (100 mHz) in Figure 5(b) was approximated to total cell resistance $R_t(= R_\Omega + R_f + R_{ct})$ and a value of about 10 kΩ was obtained. Capacitance behaviour was found at low frequencies as the phase angle became about −65° (Figure 5(b)). A total internal resistance value as large as 10 kΩ is not expected for a working battery.

The cell impedance spectrum was repeated after discharging a small portion of its available capacity and is shown in Figure 6. The data points take the shape of a single semicircle on the complex plane plot (Figure 6(a)), instead of the two expected for a Mg/electrolyte interface (Figure 4(b)). Also, the low frequency linear spike corresponding to Warburg impedance is absent. This shows that the passive film of a cell, which was subjected to minor discharge, largely constituted the measured impedance. Even though the passive film on the Mg surface had ruptured on initiating a discharge current, it appears that the coverage of the film on the surface was close to unity. Therefore, the

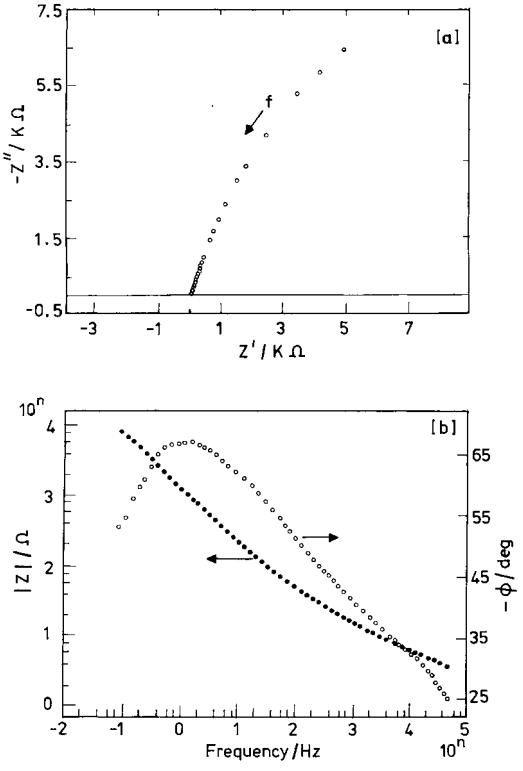

Fig. 5. Electrochemical impedance spectrum in Nyquist (a) and Bode (b) forms of an aged Mg/MnO_2 cell prior to discharge. $|Z|$, Z', Z'' and ϕ refer to modulus of impedance, real part, imaginary part and phase angle, respectively.

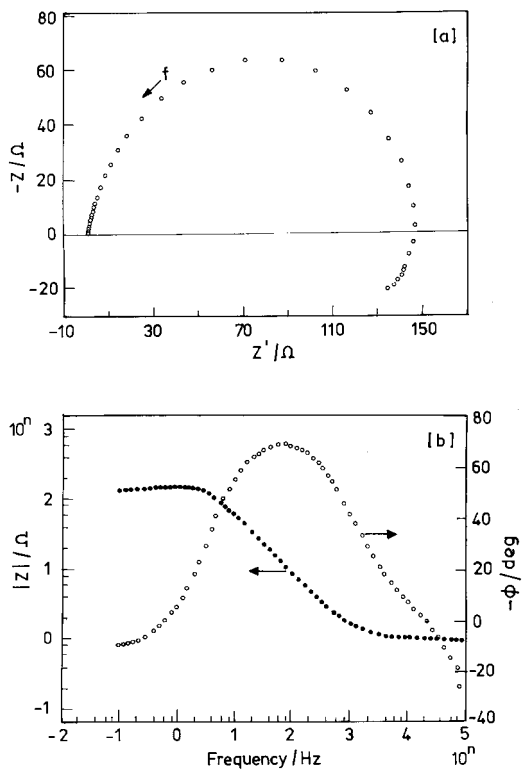

Fig. 6. Electrochemical impedance spectrum in Nyquist (a) and Bode (b) forms of a slightly discharged Mg/MnO_2 cell. Symbols as in Figure 5.

second semicircle and linear Warburg spike corresponding to film-free metal were absent. Consequently, the charge-transfer resistance (R_{ct}) of the corrosion process (Reaction 5) was high. It was, thus, inferred that the slightly discharged Mg/MnO_2 cells were likely to have high immunity to corrosion and to perforation of the Mg anode. The total internal resistance (R_t) of the cell, obtained either from the low frequency intercept of Figure 6(a) or from $|Z|$ in the low frequency region, was 140 Ω, which was much smaller than the value (10 kΩ) before discharge. The higher internal resistance before discharge was, therefore, due to the presence of a passive film on the Mg, which had grown thicker and possessed high impedance due to its long storage. The same conclusion was also evident from the voltage transient (Figure 3) in which a large voltage dip was measured during the delay-time.

The complex plane plot of a partially discharged cell (SOC ~ 0.7) contained two semicircles, which were unequal in size. As discussed earlier, the low frequency semicircle was attributed to a parallel combination of R_{ct} of Reaction 5 and the double-layer capacitance (C_{dl}) at the Mg–electrolyte interface. The fact that the low frequency semicircle was observed only after about 20–30% of the cell capacity was discharged, suggested that the coverage of the film on the Mg surface decreased with increased discharge capacity and sufficient film-free surface was exposed to the electrolyte for establishment of Reaction 5. As the low frequency linear spike was absent in all the present studies, it was inferred that the Reaction 5 was not controlled by a diffusion limited process.

Another interesting feature of the impedance spectrum was that an inductive loop appeared as shown in Figure 7, when the experiment was run in the a.c. frequency range of 100 kHz–5 mHz. This may be attributed to the porous nature of the Mg anode resulting from localized anodic oxidation through defects in the passive film.

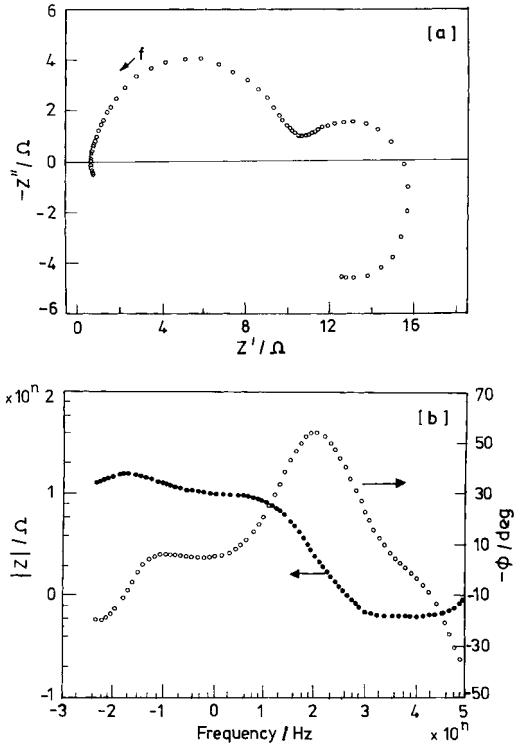

Fig. 7. Electrochemical impedance spectrum in Nyquist (a) and Bode (b) forms of a Mg/MnO_2 cell at state-of-charge ~0.7. The frequency range: 100 kHz–5 mHz. Symbols as in Figure 5.

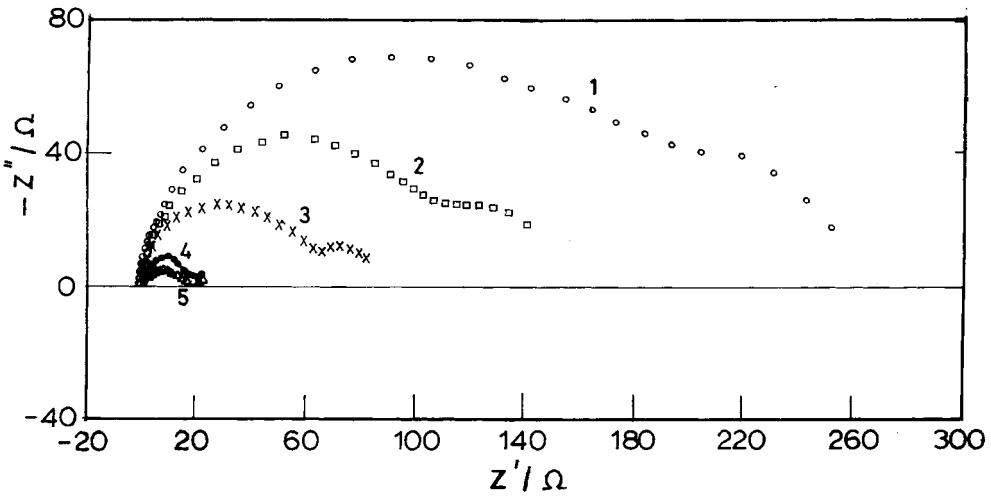

Fig. 8. Electrochemical impedance spectra of a Mg/MnO_2 cell recorded at state-of-charge ~0.97 (*1*), 0.93 (*2*), 0.90 (*3*), 0.55 (*4*) and 0.45 (*5*).

3.4. *Impedance behaviour at different states-of-charge of the cell*

Studies of impedance parameters and their dependence on state-of-charge (SOC) of batteries are of great interest [6, 8–11]. These parameters are used for non-destructive evaluation of SOC, or residual capacity of primary cells. In the present investigations, the aged Mg/MnO_2 cells were discharged and impedance spectra were recorded at different stages of discharge. The Nyquist plots recorded at different SOC values are shown in Figure 8. The plots became smaller, thus, suggesting a decreasing cell resistance as SOC decreased. To identify the SOC-sensitive impedance parameters, R_Ω, R_f, R_{ct}, R_t, f_{max}, Z' and Z'' of the high frequency semicircle were plotted as a function of SOC and are shown in Figures 9–11. The value of ohmic resistance (R_Ω) in the range between 0.6 and 0.9 Ω was almost invariant with SOC (Figure 9). There was a steep decrease in R_f from about 160 Ω to about 20 Ω during the initial stages of discharge (SOC down to 0.8), as seen in Figure 10(a). Following this, R_f decreased gradually at SOC between 0.8 and 0. It is interesting to note that the value of R_f decreased to a value as low as 5 Ω at SOC ~0. In an analogous way, R_{ct} also fell from about 85 to 20 Ω in the initial stages of discharge, and then decreased gradually to about 2 Ω at the end of discharge (Figure 10(b)). The decrease in the values of R_f, R_{ct} and also R_t (Figure 10(c)) may be attributed to a decrease in thickness and coverage of the passive film on the Mg surface; and, therefore, an increase in the area of film-free Mg. The increase in surface area is also due to formation and propagation of pores on the Mg anode due to non-uniform or localized anodic oxidation with increase in cell discharged capacity.

The variations of frequency (f_{max}) corresponding to the maximum value of the imaginary component of the

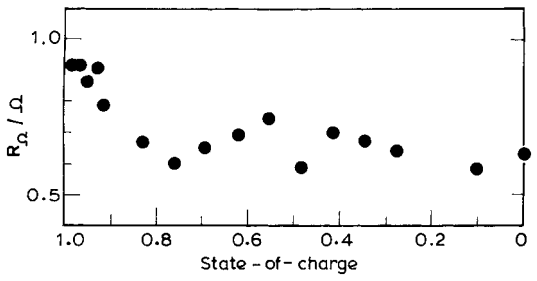

Fig. 9. Variation of ohmic resistance (R_Ω) with a decrease of state-of-charge of Mg/MnO_2 cell.

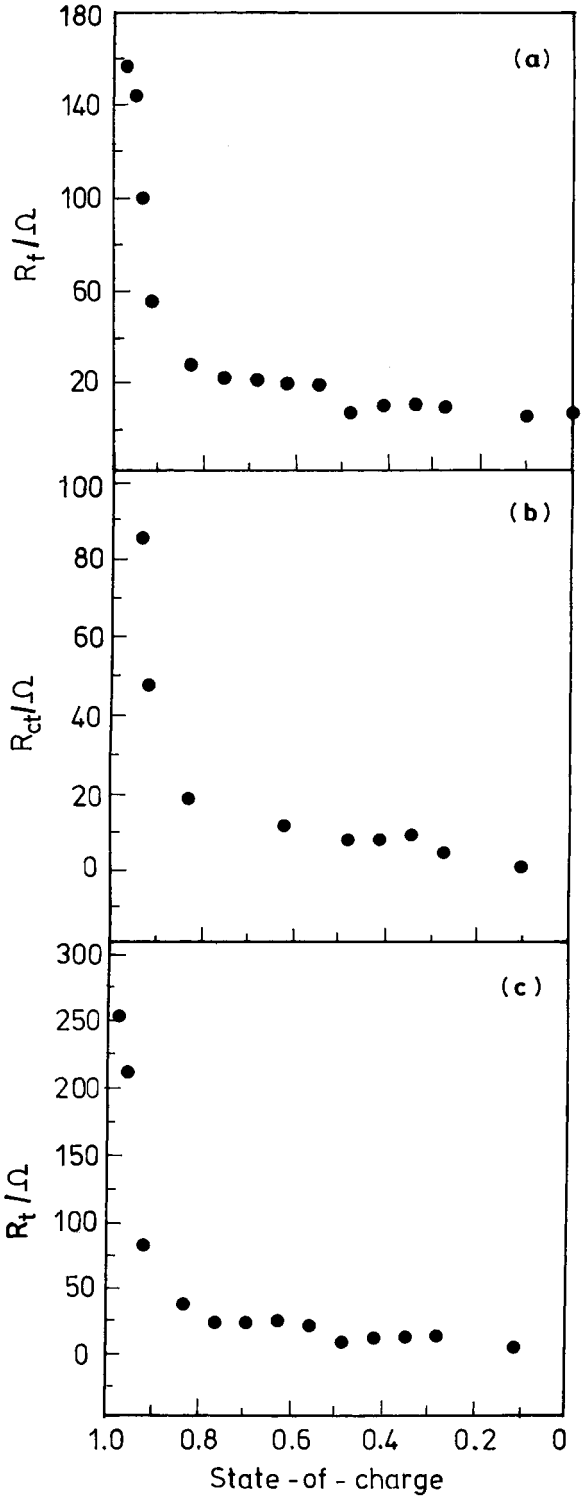

Fig. 10. Variation of resistance of passive film on Mg surface (R_f) (a), charge-transfer resistance (R_{ct}) of Reaction 5 (b) and total cell resistance (R_t) (c) as a function of decrease in state-of-charge of Mg/MnO_2 cell.

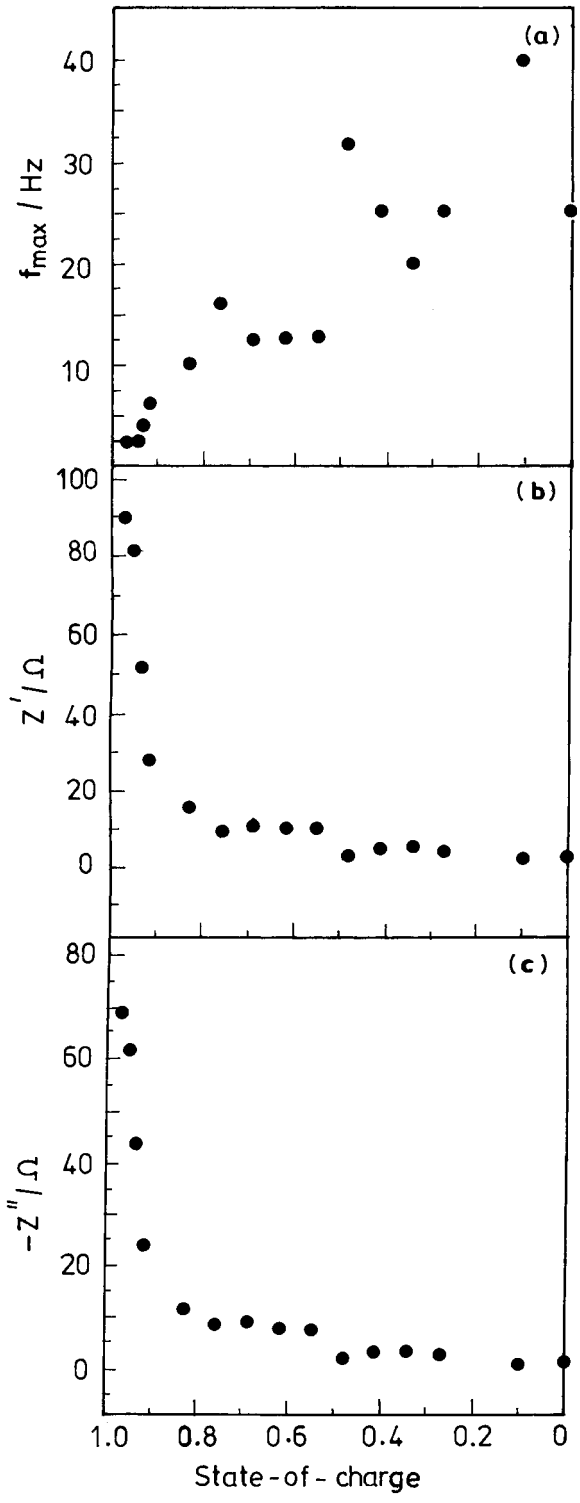

Fig. 11. Variation of frequency (f_{max}) corresponding to the maximum imaginary component of the high frequency semicircle (a), respective real component (Z') (b) and imaginary component (Z'') (c) as a function of decrease in state-of-charge of Mg/MnO_2 cell.

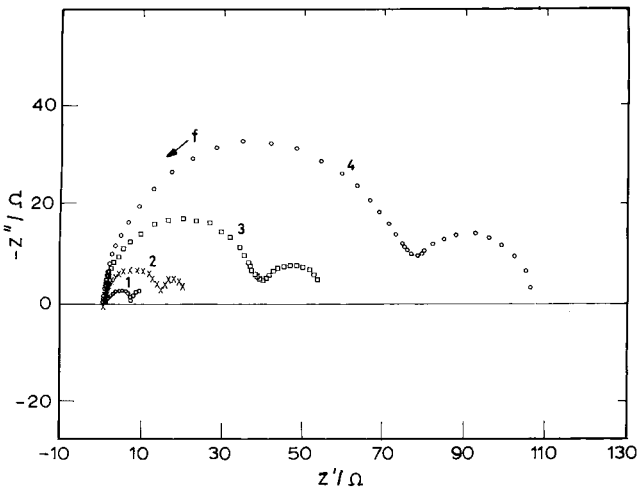

Fig. 12. Impedance spectra of a Mg/MnO_2 cell discharged to state-of-charge ~0.5. Spectra were recorded 1 (*1*), 4 (*2*), 11 (*3*) and 24 days (*4*) after the cell was discharged to state-of-charge ~0.5.

high frequency semicircle; and Z' and Z'' corresponding to f_{max} with a decrease of SOC of Mg/MnO_2 cell are shown in Figure 11. There was a steep decrease in the values of Z' and Z'' during the initial stages of cell discharge followed by a gradual decrease to the end of discharge. Although there was some scatter, f_{max} increased from about 2 Hz (an almost virgin cell) to about 40 Hz (completely used cell) (Figure 11(a)). f_{max} may be a suitable parameter for the estimate of SOC, or residual capacity, of Mg/MnO_2 cells.

3.5. *Time variation of impedance of partially discharged cell*

A Mg/MnO_2 cell was discharged to SOC ~ 0.5, and its impedance spectra were recorded at several intervals

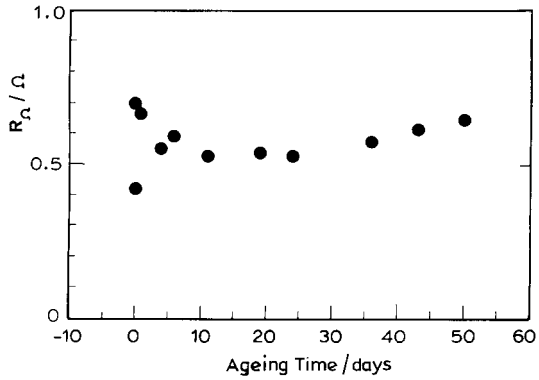

Fig. 13. Ohmic resistance (R_Ω) of a Mg/MnO_2 cell at state-of-charge ~0.5 as a function of open-circuit ageing time.

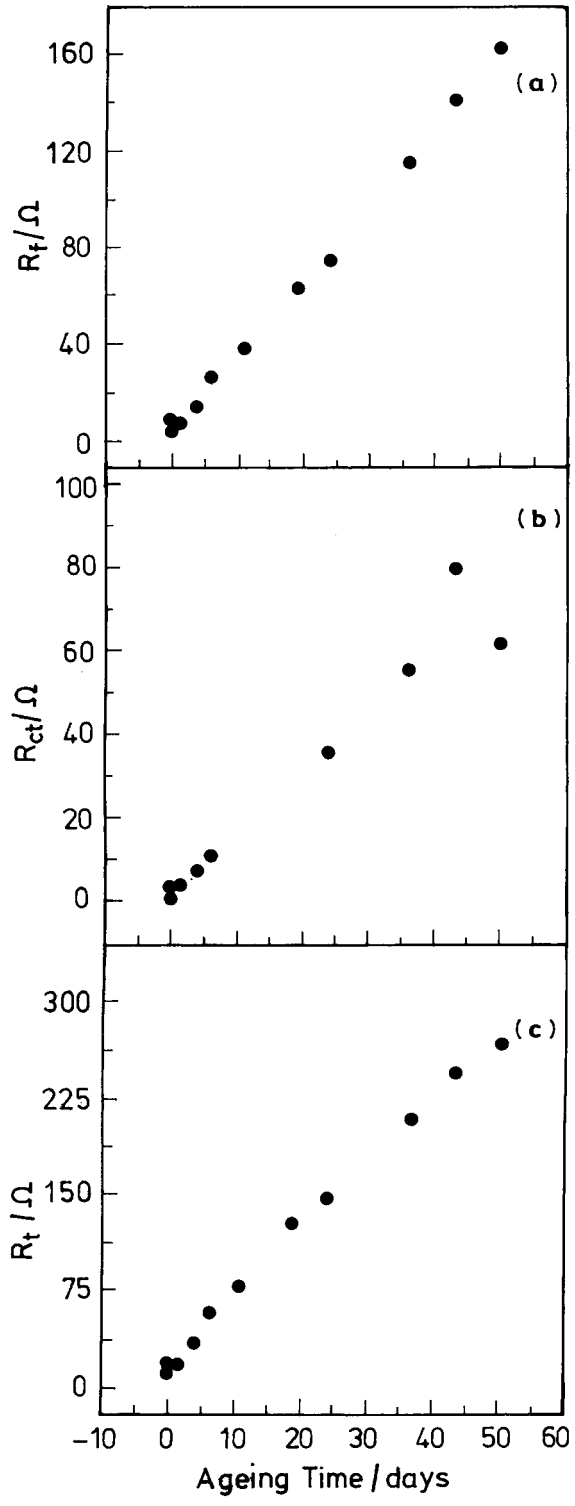

Fig. 14. Surface passive film resistance (R_f) (a), charge-transfer resistance (R_{ct}) of corrosion process (b) and total cell resistance (R_t) (c) of a Mg/MnO_2 cell at state-of-charge ~0.5 as a function of open circuit ageing time.

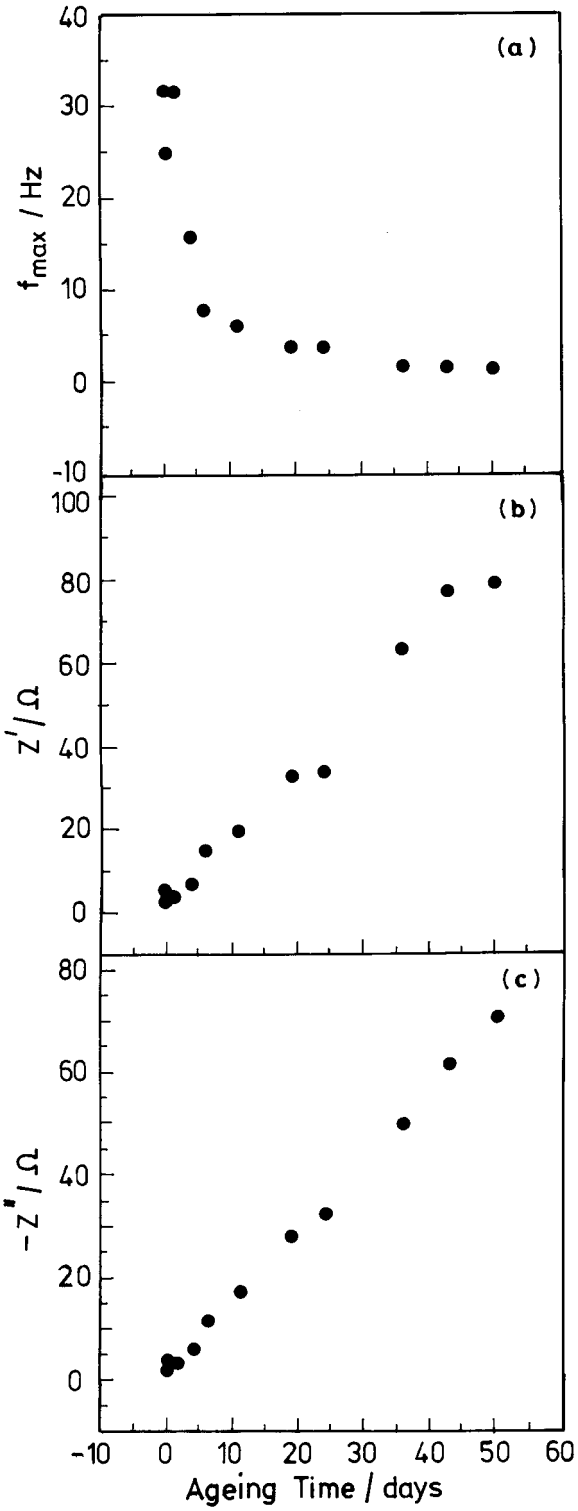

Fig. 15. Frequency (f_{max}) corresponding to the maximum value of imaginary component of high frequency semicircle (a), respective real component (Z') (b) and imaginary component (Z'') (c) of a Mg/MnO_2 cell at state-of-charge ~0.5 as a function of open circuit ageing time.

during open-circuit storage for several days. These measurements were considered to be important in view of the build-up of a highly resistive passive film on the Mg anode during long periods of storage. Some of the impedance spectra are shown in Figure 12 as complex plane plots. The size of the spectrum gradually increased over a duration of about 50 days. The changes with time of the impedance parameters are shown in Figures 13–15. The ohmic resistance (R_Ω) of the cell remained almost invariant at about 0.6 Ω (Figure 13). The values of R_f, R_{ct} and R_t (Figure 14) and also Z' and Z'' (Figure 15) increased linearly with ageing time. The behaviour of these parameters reflected a linear growth of the passive film on the Mg surface and a concomitant decrease in the corrosion rate of the Mg (increase of R_{ct}). There was a rapid decrease in the value of f_{max} (Figure 16(a)) during the initial stages of storage of a partially discharged Mg/MnO_2 cell, followed by a slow decrease. Thus, the impedance parameters discussed above, except f_{max}, may be useful in predicting the age of a Mg/MnO_2 cell.

4. Conclusions

Mg/MnO_2 cells were shown to possess a long shelf life. The cells retained significant capacity even a decade after cell assembly. The cells were free from perforations, and the open-circuit voltage was almost the same as the voltage of freshly assembled cells. The dip in cell voltage on initiation of discharge, however, was found to be rather large with a marginal increase in delay time. Although the total resistance of an undischarged cell was extremely high, it decreased to a low value following breakdown of the passive film. The cell resistance was found to be as low as 7 Ω at the end of discharge. The impedance parameters were shown to depend on the SOC of the cell. The frequency, f_{max}, corresponding to the maximum value of the imaginary component of high frequency semicircle, was identified as a useful parameter to predict the SOC of the cell. The time variation of the impedance of a partially discharged cell revealed an increase in the magnitude of resistance parameters. This feature was attributed to the growth of a passivating layer on the Mg surface and a decrease in the corrosion rate of Mg.

Acknowledgements

The author is thankful to N. Radhika for her assistance in some of the experiments.

References

1. J.L. Robinson, *in* 'The Primary Battery', vol. 2 edited by N.C. Cahoon and G.W. Heise (J. Wiley & Sons, New York, 1976), p. 149.
2. S.R. Narayanan and S. Sathyanarayana, *J. Power Sources* **15** (1985) 27.
3. S.R. Narayanan and S. Sathyanarayana, *J. Power Sources* **24** (1988) 51.
4. S.R. Narayanan and S. Sathyanarayana, *J. Power Sources* **24** (1988) 295.
5. B.V. Ratna Kumar and S. Sathyanarayana, *J. Power Sources* **10** (1983) 219.
6. M.J. Root, *J. Appl. Electrochem.* **25** (1995) 1057.
7. J.E.B. Randles, *Discuss. Faraday Soc.* **1** (1947) 111.
8. S.A.G.R. Karunathilaka, N.A. Hampson, R. Leek and T.J. Sinclair, *J. Appl. Electrochem.* **10** (1980) 357.
9. S.A.G.R. Karunathilaka, N.A. Hampson, R. Leek and T.J. Sinclair, *J. Appl. Electrochem.* **10** (1980) 603.
10. S.A.G.R. Karunathilaka, N.A. Hampson, R. Leek and T.J. Sinclair, *J. Appl. Electrochem.* **10** (1980) 799.
11. M.L. Gopikanth and S. Sathyanarayana, *J. Appl. Electrochem.* **9** (1979) 581.